GEOLOGY | THE GEOLOGICAL SOCIETY OF AMERICA®

https://doi.org/10.1130/G46431.1

Manuscript received 18 April 2019
Revised manuscript received 17 September 2019
Manuscript accepted 18 September 2019

Published online 28 October 2019

Calcium isotope evidence for environmental variability before and across the Cretaceous-Paleogene mass extinction

Benjamin J. Linzmeier[1], Andrew D. Jacobson[1], Bradley B. Sageman[1], Matthew T. Hurtgen[1], Meagan E. Ankney[1], Sierra V. Petersen[2], Thomas S. Tobin[3], Gabriella D. Kitch[1] and Jiuyuan Wang[1]

[1]Department of Earth and Planetary Sciences, Northwestern University, 2145 Sheridan Road, Evanston, Illinois 60208, USA
[2]Earth and Environmental Sciences Department, University of Michigan, 1100 N. University Avenue, Ann Arbor, Michigan 48109, USA
[3]Department of Geological Sciences, The University of Alabama, 201 7th Avenue, Tuscaloosa, Alabama 35487, USA

ABSTRACT

Carbon dioxide release during Deccan Traps volcanism and the Chicxulub impact likely contributed to the Cretaceous-Paleogene (K-Pg) mass extinction; however, the intensity and duration of CO_2 input differed between the two events. Large and rapid addition of CO_2 to seawater causes transient decreases in pH, [CO_3^{2-}], and carbonate mineral saturation states. Compensating mechanisms, such as dissolution of seafloor sediment, reduced biomineralization, and silicate weathering, mitigate these effects by increasing the same parameters. The calcium isotope ratios ($\delta^{44/40}$Ca) of seawater and marine carbonates are hypothesized to respond to these perturbations through weathering/carbonate deposition flux imbalances and/or changes in fractionation between carbonate minerals and seawater. We used a high-precision thermal ionization mass spectrometry method to measure $\delta^{44/40}$Ca values of aragonitic bivalve and gastropod mollusk shells from the K-Pg interval of the López de Bertodano Formation on Seymour Island, Antarctica. Well-preserved shells spanning the late Maastrichtian (ca. 67 Ma) to early Danian (ca. 65.5 Ma) have $\delta^{44/40}$Ca values ranging from −1.89‰ to −1.57‰ (seawater [sw]). Shifts in $\delta^{44/40}$Ca inversely correlate with sedimentological indicators of saturation state. A negative excursion begins before and continues across the K-Pg boundary. According to a simple mass-balance model, neither input/output flux imbalances nor change in the globally integrated bulk carbonate fractionation factor can produce variations in seawater $\delta^{44/40}$Ca sufficient to explain the measured trends. The data are consistent with a dynamic molluscan Ca isotope fractionation factor sensitive to the carbonate geochemistry of seawater. The K-Pg extinction appears to have occurred during a period of carbonate saturation state variability caused by Deccan volcanism.

INTRODUCTION

Debate persists about the causes of the Cretaceous-Paleogene (K-Pg) mass extinction. The bolide impact at Chicxulub left a globally distributed iridium anomaly at the primary extinction horizon that is coincident with the rapid extinction of both terrestrial and marine organisms (Schulte et al., 2010; Lyson et al., 2011; Witts et al., 2016). Some propose that eruption of the Deccan Traps large igneous province (LIP) caused the extinction (Keller et al., 2009). Although LIP volcanism commonly corresponds with mass extinctions (Clapham and Renne, 2019), questions remain about the link between Deccan volcanism and the K-Pg extinction, given the magnitude and timing of eruptions (Schoene et al., 2019; Sprain et al., 2019).

Deccan volcanism released large quantities of CO_2 (Nordt et al., 2003), which likely caused warming (Petersen et al., 2016; Barnet et al., 2018) and ocean acidification (OA; Henehan et al., 2016; Dameron et al., 2017). OA, which encompasses transient decreases in pH, [CO_3^{2-}], and carbonate mineral saturation states resulting from the large and rapid injection of CO_2 into the atmosphere-ocean system, may have caused extinctions throughout Earth history (Hönisch et al., 2012). Sedimentological indicators, such as reduced carbonate weight percent and increased planktic foraminiferal fragmentation, suggest eruption of the Deccan Traps forced OA before the K-Pg boundary (Henehan et al., 2016; Dameron et al., 2017). The bolide impact may have caused lesser and transient OA (e.g., 1–10 yr; Tyrrell et al., 2015). During and following OA, dissolution of seafloor carbonate (Ridgwell and Zeebe, 2005) and biological compensation (Boudreau et al., 2018) restore balance by neutralizing acidity and elevating alkalinity. Over longer time scales, silicate weathering plays a similar role (Ridgwell and Zeebe, 2005; Blättler and Higgins, 2017).

The calcium isotope system offers a valuable proxy for detecting OA in deep time (Payne et al., 2010). The $\delta^{44/40}$Ca values of seawater ($\delta^{44/40}Ca_{sw}$) and carbonate sediment are sensitive to the balance between weathering inputs and carbonate output (Fantle, 2010), carbonate mineralogy (Blättler et al., 2012), and changes in isotopic fractionation during primary carbonate mineral production (Du Vivier et al., 2015). To determine if Deccan volcanism or the bolide impact perturbed ocean carbonate chemistry, we measured the $\delta^{44/40}$Ca of aragonitic mollusks from Seymour Island, Antarctica (Fig. 1), that span the late Maastrichtian to the earliest Danian interval.

MATERIALS AND METHODS

Geological Setting

The López de Bertodano Formation was deposited in the James Ross Basin, in an open-ocean–facing shelf environment with water depths near 150 m (Huber, 1988). The formation consists of siliciclastic clays and silts with interspersed sand beds and carbonate concretions. Sedimentation rates were high (10–30 cm/k.y.; Tobin et al., 2012; Witts et al., 2015). We applied a linear age model between magnetostratigraphic reversals (C30r-C30n-C29r-C29n [r—reverse, n—normal]) and the K-Pg boundary horizon using Ar-Ar ages from Sprain et al. (2018). An age model uncertainty of ~13–40 k.y. was estimated by comparing the stratigraphic thicknesses of molluscan units (defined by Macellari, 1988) in measured sections (Tobin et al., 2012) with

CITATION: Linzmeier, B.J., et al., 2020, Calcium isotope evidence for environmental variability before and across the Cretaceous-Paleogene mass extinction: Geology, v. 48, p. 34–38, https://doi.org/10.1130/G46431.1

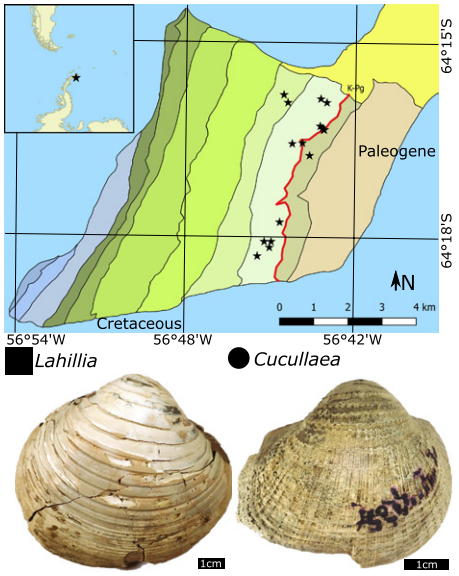

Figure 1. Map of Seymour Island, Antarctica (after Schoepfer et al., 2017) with fossil collection localities and example shells of *Lahillia* (left) and *Cucullaea* (right) analyzed in this study. Green colored zones are informal subdivisions of the López de Bertodano Formation (Macellari, 1988). Stratigraphic positioning of fossils shown on map was done by plane projection (Zinsmeister, 2001), which corresponds well to fossils measured in stratigraphic distance to the Cretaceous-Paleogene (K-Pg) boundary (Witts et al., 2016; Petersen et al., 2016; Tobin, 2017).

those derived from plane projection (Zinsmeister, 2001). Correlation to other sections and the Deccan eruption estimates relied on the magnetostratigraphic reversal horizons and the K-Pg horizon, with linear age scaling between these horizons. For more explanation of the age model, see the extended description of the geological setting in the GSA Data Repository[1].

Materials

Analyses included samples from 23 horizons. Most shells were from bivalves (Fig. 1; Table DR1 in the Data Repository) of the genera *Lahillia* ($n = 26$) and *Cucullaea* ($n = 9$). Two *Amberleya* gastropods and four samples of carbonate cement from sediment attached to shells were also measured (Fig. 2). Sampling of shells combined multiple years of growth (Petersen et al., 2016) and averaged potential seasonal variation in $\delta^{44/40}$Ca (Hippler et al., 2013). *Lahillia* and *Cucullaea* were shallow infauna that recorded δ^{18}O from seawater rather than pore water (Hall et al., 2018), so shell $\delta^{44/40}$Ca most likely reflects a seawater source. *Amberleya* was a slow motile epifaunal surface deposit–feeding gastropod with similar characteristics (Witts et al., 2016).

Analytical Methods

Elemental and isotopic analyses were performed at Northwestern University (Illinois, USA). Elemental analyses by inductively coupled plasma–optical emission spectrometry (ICP-OES) have an uncertainty of ± 5%. Calcium isotope ratios (^{44}Ca/^{40}Ca) were measured using a high-precision ^{43}Ca-^{42}Ca double-spike thermal ionization mass spectrometry (TIMS) technique (Lehn et al., 2013). Results are reported in delta notation ($\delta^{44/40}$Ca) relative to the Ocean Scientific International Ltd. (OSIL) seawater (SW) standard. During the period of study, analyses of OSIL SW and U.S. National Institute of Standards and Technology (NIST) 915b (calcium carbonate) yielded mean $\delta^{44/40}$Ca values of 0.000 ± 0.009‰ (2 standard error of the mean [SEM], $n = 37$) and − 1.130‰ ± 0.016‰ (2 SEM, $n = 10$). These results correspond to a short-term, external reproducibility of ± 0.05‰ (2 standard deviation [SD]), which is the uncertainty adopted here. Replicate analyses of the same shells produced an average range of 0.03‰, and replicates of different shells within horizons produced an average range of 0.04‰. Radiogenic strontium isotope ratios (^{87}Sr/^{86}Sr) were also analyzed by TIMS (Andrews et al., 2016). Analyses of U.S. National Bureau of Standards (NBS) 987 (strontium carbonate) yielded a ^{87}Sr/^{86}Sr ratio of 0.710252 ± 0.000008 (2 SD, $n = 5$). See the extended analytical methods in the Data Repository for more details, as well as Tables DR4 and DR5 for TIMS and ICP-OES data.

RESULTS AND DISCUSSION

Sample $\delta^{44/40}$Ca values ranged between −2.25‰ and −0.82‰, with carbonate cement having much higher values than shells (Fig. 2A). Changes through stratigraphy also exist (Fig. 3A). Temperatures calculated from Δ_{47} do not correlate with $\delta^{44/40}$Ca for 13 shells with paired analyses (Fig. 2B). Different mollusks from the same or closely spaced horizons yielded similar $\delta^{44/40}$Ca values (Fig. 3A), suggesting no species-specific "vital effects." Variations in $\delta^{44/40}$Ca coincide with excursions in sedimentological indicators of carbonate saturation from globally distributed locations (Fig. 3C), which presumably reflect fluctuations in seawater pH and [CO_3^{2-}] forced by volcanic CO_2 emissions (Fig. 3E).

Diagenesis of $\delta^{44/40}$Ca in Mollusks

Diagenetic alteration of aragonitic mollusk shells can increase Sr/Ca and change O and Sr isotope ratios, even when original mineralogy is mostly preserved (Cochran et al., 2010). Three shells showing the highest Sr/Ca have lower $\delta^{44/40}$Ca than shells with low Sr/Ca from the same horizons (Fig. 2A; Fig. DR1). Diagenesis of aragonitic mollusk shells appears to affect $\delta^{44/40}$Ca differently compared to bulk carbonate sediments and microfossils, where progressive alteration decreases Sr/Ca and increases $\delta^{44/40}$Ca (Higgins et al., 2018). We excluded these shells with anomalously high Sr/Ca from further interpretation, similar to previous studies (Tobin et al., 2012; Petersen et al., 2016).

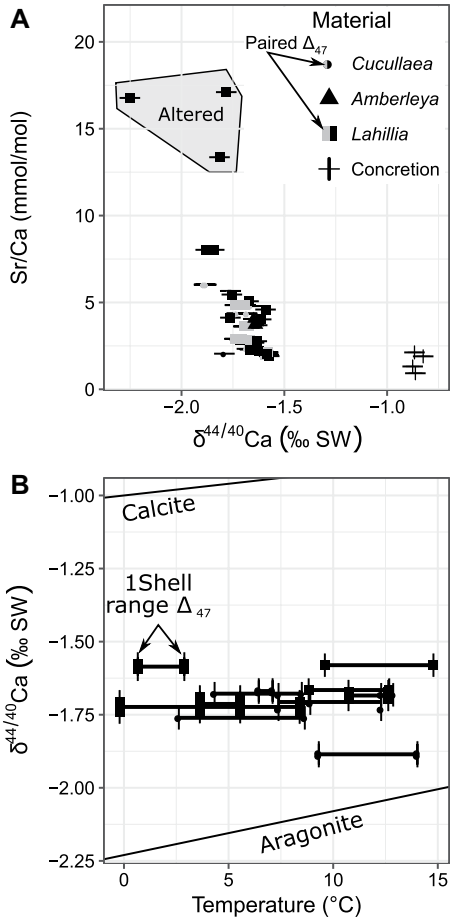

Figure 2. Comparisons among $\delta^{44/40}$Ca, Sr/Ca, and Δ_{47}-based temperatures. (A) $\delta^{44/40}$Ca versus Sr/Ca for the complete data set highlighting a subset of mollusks with paired Δ_{47}-based temperatures. Note three shells with the highest Sr/Ca were removed from later discussion; concretion calcite has the lowest Sr/Ca and highest $\delta^{44/40}$Ca measured. SW—seawater. (B) Δ_{47}-based temperatures (Petersen et al., 2016) versus $\delta^{44/40}$Ca for 13 bivalves. Horizontal bars span the range of temperatures calculated from two measurements of each shell and connect mean $\delta^{44/40}$Ca. Replicate analyses of $\delta^{44/40}$Ca are plotted at the end of each bar. Temperature dependence of $\delta^{44/40}$Ca fractionation in inorganic carbonates is shown for reference (Gussone et al., 2003; Marriott et al., 2004).

Controls on $\delta^{44/40}$Ca Variation Through Time

Secular Evolution of $\delta^{44/40}Ca_{sw}$

One hypothesis to explain the observed record is that the mollusk fractionation factor

[1]GSA Data Repository item 2020008, data tables, figures, age models, description of modeling, and extended discussion, is available online at http://www.geosociety.org/datarepository/2020/, or on request from editing@geosociety.org.

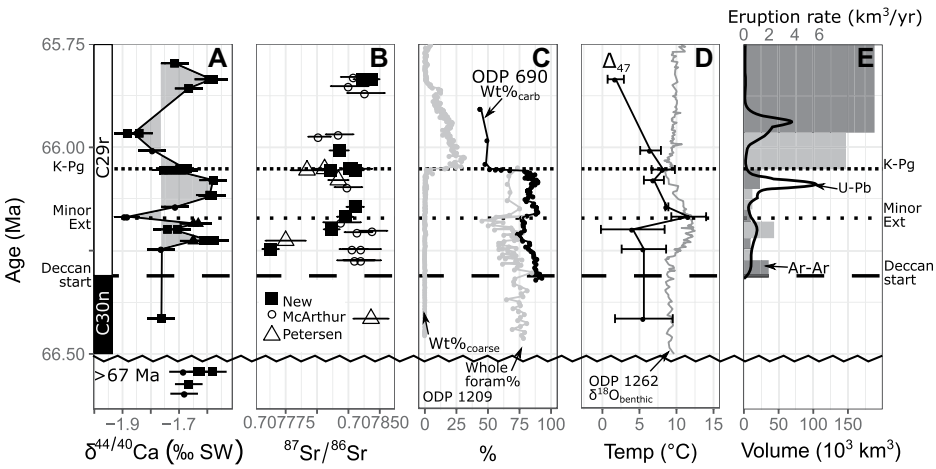

Figure 3. Stratigraphic distribution of $\delta^{44/40}Ca$ values through the section at Seymour Island, Antarctica, compared to other local and global data sets. Horizontal dashed and dotted lines correspond to the initiation of Deccan Traps volcanism, a minor putative local extinction (Tobin, 2017), and the Cretaceous-Paleogene (K-Pg) boundary. (A) Mollusk $\delta^{44/40}Ca$ values from samples in this study showing variation through time; same symbols as used in Figure 2; SW—seawater. (B) Minimal change in $^{87}Sr/^{86}Sr$ suggests uniform weathering rates (this study; mollusk data from McArthur et al., 1998; Petersen et al., 2016). (C) Sedimentological indicators (carbonate wt%, coarse fraction, and foraminiferal fragmentation percent) of ocean acidification (OA) from Ocean Drilling Program (ODP) Site 690 (Maud Rise near Antarctica; data from Ehrendorfer, 1993; O'Connell, 1990) and Site 1209 (Shatsky Rise, equatorial Pacific; data from Westerhold et al., 2011; Henehan et al., 2016). (D) Seymour Island mollusk Δ_{47}-based temperatures (Petersen et al., 2016) and deep-sea foraminifera $\delta^{18}O$-based temperatures (gray line) from ODP Site 1262 (Angola Basin; Barnet et al., 2018). (E) Flow volumes and timing from Sprain et al. (2019). Eruption rate and timing estimates are from Schoene et al. (2019).

($\Delta^{44/40}Ca_{shell\text{-}sw}$) remained constant while $\delta^{44/40}Ca_{sw}$ changed (Fig. 4). Imbalances between calcium input and output fluxes, as well as changes in the isotope fractionation factor between seawater and globally integrated carbonate sediment, offer the most plausible mechanisms for shifting $\delta^{44/40}Ca_{sw}$ (Fantle, 2010). Seawater [Ca] values, and residence time by extension, determine the shape, magnitude, and duration of $\delta^{44/40}Ca_{sw}$ excursions (Fig. 4). Nearly uniform $^{87}Sr/^{86}Sr$ ratios through the study interval suggest stable weathering inputs (Fig. 3B), whereas variable carbonate weight percent ($wt\%_{carb}$) data from deep-sea cores indicate fluctuating carbonate output (Fig. 3C).

A simple flux-balance model forced by scaling the carbonate burial flux according to Ocean Drilling Program (ODP) Site 690 (southwestern flank of Maud Rise) $wt\%_{carb}$ values produces maximum estimates of $\delta^{44/40}Ca_{sw}$ variation (Fig. 4; see the Data Repository for details). To establish an initial steady state, the weathering flux (F_w) was set equal to the carbonate burial flux, which was modeled as the total ocean Ca mass in moles (N_{Ca}) divided by residence time (τ_{Ca}). Ocean [Ca] values were set at the limits of estimated ranges for Late Cretaceous seawater (~10–50 mmol/kg; Lasaga et al., 1985; Wallmann, 2001), and residence time was scaled to maintain initial steady state with a fixed weathering flux. The carbonate output flux was then scaled by the carbonate weight percent ($wt\%_{carb}$) based on change from initial conditions (i) using smoothed data from ODP Site 690 (O'Connell, 1990; Ehrendorfer, 1993). The model equations are:

$$\frac{dN_{Ca}}{dt} = F_w - \frac{wt_{carb_t}}{wt_{carb_i}} * \frac{N_{Ca_t}}{\tau_{Ca}}, \quad (1)$$

$$\frac{d\left(N_{Ca}\delta_{sw}\right)}{dt} = F_w * \delta_W - \left(\delta_{sw} + \Delta_c\right) * \frac{wt_{carb_t}}{wt_{carb_i}} * \frac{N_{Ca_t}}{\tau_{Ca}}, \quad (2)$$

where δ_{sw} and δ_w represent the $\delta^{44/40}Ca$ values of seawater and the weathering flux, respectively, and Δ_c is the average fractionation factor of global carbonate output. Model calculations predict almost no change before the K-Pg boundary and a gradual shift (>–0.10‰) at the K-Pg boundary only when low [Ca] values are assumed (Fig. 4). Models that explicitly incorporate carbonate chemistry would yield even smaller changes (Komar and Zeebe, 2016). Shifts in the global fractionation factor between seawater and bulk carbonate sediment ranging up to 1.0‰ also fail to reproduce the magnitude or direction of $\delta^{44/40}Ca_{SW}$ change required to explain the mollusk record (Fig. DR4). As with flux imbalances, high [Ca] values mask perturbations from small shifts in fractionation and dampen those from larger ones.

Mollusk $\delta^{44/40}Ca$ Fractionation Factor

If $\delta^{44/40}Ca_{sw}$ did not significantly vary though this interval, then $\Delta^{44/40}Ca_{shell\text{-}sw}$ must have changed (Fig. 4). Research examining carbonate precipitation predicts less fractionation, and hence positive $\delta^{44/40}Ca$ excursions, during decreased saturation and vice versa during increased saturation (Tang et al., 2008; Kısakürek et al., 2011; Nielsen et al., 2012; Mejía et al., 2018). The mollusk $\delta^{44/40}Ca$ record illustrates such a pattern when evaluated against sedimentological proxies for saturation state (Figs. 3A and 3C). In mollusks, fractionation likely occurs during Ca transport into the extrapallial fluid (EPF) from which the shell precipitates, as some buffering of the EPF occurs across a range of seawater pH and pCO_2 conditions (Heinemann et al., 2012). Ion-selective intracellular channels transport most of the Ca into the EPF, where biomineralization rates regulate concentration gradients with surrounding seawater, which in turn control the magnitude of diffusive fluxes across membranes (Carré et al., 2006). Passive, nonselective intercellular pathway diffusion and active enzymatic (Ca^{2+}-ATPase and carbonic anhydrase) pumping may also elicit isotope fractionation (Carré et al., 2006). Carbonate chemistry could affect $\Delta^{44/40}Ca_{shell\text{-}sw}$ by altering one pathway or changing the relative balance among the three, although the exact fractionation mechanisms remain unknown (Gussone

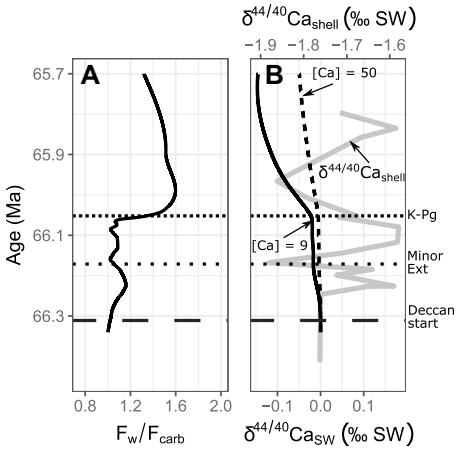

Figure 4. Forward modeling of $\delta^{44/40}Ca_{sw}$ (sw—seawater) variation across a range of [Ca] driven by flux imbalance. Seawater Ca concentrations for the Cretaceous-Paleogene (K-Pg) ranged from 9 to 50 mmol/kg (Lasaga et al., 1985; Wallmann, 2001). (A) Flux estimates based on scaling burial flux of carbonate (F_{carb}) using carbonate content ($wt\%_{carb}$) at Ocean Drilling Program (ODP) Site 690 (Maud Rise near Antarctica) assuming constant weathering flux (F_w). (B) Modeled $\delta^{44/40}Ca_{sw}$ compared to measured $\delta^{44/40}Ca$ (gray line) showing that variation before the K-Pg was much larger than predicted from flux imbalances alone, and the excursion across the boundary is only partially predicted when low [Ca] values are assumed.

and Heuser, 2016; see the Data Repository for an extended discussion of biomineralization).

Implications for the Mass Extinction

Our high-precision $\delta^{44/40}$Ca record through the K-Pg mass extinction displays considerable complexity (Fig. 3A) driven by the response of biocalcifiers to volcanic CO_2 outgassing. In particular, the short time scales of carbonate saturation state variation point to biotic compensation rather than chemical compensation as the dampening mechanism to OA (Boudreau et al., 2018). The first positive excursion corresponds to deep-sea warming and may indicate reduced saturation from CO_2 outgassing that was independent of the size of Deccan flows (Fig. 3). The first negative excursion lags increased flow size (Fig. 3E) but coincides with increased carbonate export (Fig. 3C) and a local extinction identified by statistical analysis of fossil occurrences (Tobin, 2017). The minor extinction may relate to water depth change (Witts et al., 2016). The second positive excursion indicates a return to lower saturation due to either biocalcification recovery or renewed OA. Volcanic CO_2 inputs may have prolonged this excursion and stressed biocalcifiers, eventually causing increased carbonate saturation and thereby the negative excursion that begins below the K-Pg boundary (Fig. 3A). If the foraminiferal "dissolution facies" of Huber (1988) is due to OA, then an additional positive $\delta^{44/40}$Ca excursion may be found in mollusks recovered from low in this interval. In total, our data suggest that Deccan volcanism perturbed ocean carbonate chemistry before the K-Pg boundary and further support the hypothesis that the combined effect of Deccan volcanism and the Chicxulub impact may have been necessary to drive the K-Pg mass extinction (Arens and West, 2008).

CONCLUSIONS

Mollusk shells from Seymour Island, Antarctica, show analytically resolvable $\delta^{44/40}$Ca variations before and across the K-Pg boundary. We found that diagenetic alteration drives molluscan aragonite $\delta^{44/40}$Ca lower—with increasing Sr/Ca—rather than converging on cement calcite values. Neither temperature nor species-specific vital effects explain the changes in the $\delta^{44/40}$Ca of well-preserved shells. Similarly, neither input/output flux imbalances nor changes in the global fractionation factor ascribed to bulk carbonate sediment can reproduce shifts in the mollusk record, given high Late Cretaceous seawater Ca concentrations, as well as the geologically instantaneous time scale over which the shifts occurred. We propose that mollusk $\Delta^{44/40}Ca_{shell\text{-}sw}$ is dynamic. Negative $\delta^{44/40}$Ca shifts coincide with globally distributed sedimentological indicators of increased carbonate mineral saturation and vice versa for positive shifts. Calcium isotope variability before and crossing the K-Pg boundary suggests that the bolide impact coincided with preexisting carbon cycle instability resulting from Deccan volcanism and may have occurred during a phase of carbonate saturation increase due to biocalcification stress.

ACKNOWLEDGMENTS

We thank the field team for sample collection, and the crews of the R/V *Nathaniel B. Palmer*, R/V *Laurence M. Gould*, and Air Center Helicopters (Texas, USA) for logistical support. The study benefited from discussions with J.D. Witts and R. Mohr, as well as input from two anonymous reviewers. The following funding sources supported this research: the Ubben Program for Climate and Carbon Science at Northwestern University (Illinois, USA), the David and Lucile Packard Foundation (2007–31757), U.S. National Science Foundation (NSF) grant EAR-0723151, and NSF grants ANT-1341729, ANT-0739541, and ANT-0739432.

REFERENCES CITED

Andrews, M.G., Jacobson, A.D., Lehn, G.O., Horton, T.W., and Craw, D., 2016, Radiogenic and stable Sr isotope ratios ($^{87}Sr/^{86}Sr$, $\delta^{88}/^{86}Sr$) as tracers of riverine cation sources and biogeochemical cycling in the Milford Sound region of Fiordland, New Zealand: Geochimica et Cosmochimica Acta, v. 173, p. 284–303, https://doi.org/10.1016/j.gca.2015.10.005.

Arens, N.C., and West, I.D., 2008, Press-pulse: A general theory of mass extinction?: Paleobiology, v. 34, p. 456–471, https://doi.org/10.1666/07034.1.

Barnet, J.S.K., Littler, K., Kroon, D., Leng, M.J., Westerhold, T., Röhl, U., and Zachos, J.C., 2018, A new high-resolution chronology for the late Maastrichtian warming event: Establishing robust temporal links with the onset of Deccan volcanism: Geology, v. 46, p. 147–150, https://doi.org/10.1130/G39771.1.

Blättler, C.L., and Higgins, J.A., 2017, Testing Urey's carbonate-silicate cycle using the calcium isotopic composition of sedimentary carbonates: Earth and Planetary Science Letters, v. 479, p. 241–251, https://doi.org/10.1016/j.epsl.2017.09.033.

Blättler, C.L., Henderson, G.M., and Jenkyns, H.C., 2012, Explaining the Phanerozoic Ca isotope history of seawater: Geology, v. 40, p. 843–846, https://doi.org/10.1130/G33191.1.

Boudreau, B.P., Middelburg, J.J., and Luo, Y., 2018, The role of calcification in carbonate compensation: Nature Geoscience, v. 11, p. 894, https://doi.org/10.1038/s41561-018-0259-5.

Carré, M., Bentaleb, I., Bruguier, O., Ordinola, E., Barrett, N.T., and Fontugne, M., 2006, Calcification rate influence on trace element concentrations in aragonitic bivalve shells: Evidences and mechanisms: Geochimica et Cosmochimica Acta, v. 70, p. 4906–4920, https://doi.org/10.1016/j.gca.2006.07.019.

Clapham, M.E., and Renne, P.R., 2019, Flood basalts and mass extinctions: Annual Review of Earth and Planetary Sciences, v. 47, p. 275–303, https://doi.org/10.1146/annurev-earth-053018-060136.

Cochran, J.K., Kallenberg, K., Landman, N.H., Harries, P.J., Weinreb, D., Turekian, K.K., Beck, A.J., and Cobban, W.A., 2010, Effect of diagenesis on the Sr, O, and C isotope composition of Late Cretaceous mollusks from the Western Interior Seaway of North America: American Journal of Science, v. 310, p. 69–88, https://doi.org/10.2475/02.2010.01.

Dameron, S.N., Leckie, R.M., Clark, K., MacLeod, K.G., Thomas, D.J., and Lees, J.A., 2017, Extinction, dissolution, and possible ocean acidification prior to the Cretaceous/Paleogene (K/Pg) boundary in the tropical Pacific: Palaeogeography, Palaeoclimatology, Palaeoecology, v. 485, p. 433–454, https://doi.org/10.1016/j.palaeo.2017.06.032.

Du Vivier, A.D.C., Jacobson, A.D., Lehn, G.O., Selby, D., Hurtgen, M.T., and Sageman, B.B., 2015, Ca isotope stratigraphy across the Cenomanian–Turonian OAE 2: Links between volcanism, seawater geochemistry, and the carbonate fractionation factor: Earth and Planetary Science Letters, v. 416, p. 121–131, https://doi.org/10.1016/j.epsl.2015.02.001.

Ehrendorfer, T.W., 1993, Late Cretaceous (Maestrichtian) Calcareous Nannoplankton Biogeography with Emphasis on Events Immediately Preceding the Cretaceous/Paleocene Boundary [Ph.D. thesis]: Cambridge, Massachusetts, Massachusetts Institute of Technology, 288 p., https://doi.org/10.1575/1912/5508.

Fantle, M.S., 2010, Evaluating the Ca isotope proxy: American Journal of Science, v. 310, p. 194–230, https://doi.org/10.2475/03.2010.03.

Gussone, N., and Heuser, A., 2016, Biominerals and biomaterial, *in* Gussone, N., et al., eds., Calcium Stable Isotope Geochemistry: Berlin, Springer, p. 111–144, https://doi.org/10.1007/978-3-540-68953-9_4.

Gussone, N., Eisenhauer, A., Heuser, A., Dietzel, M., Bock, B., Böhm, F., Spero, H.J., Lea, D.W., Bijma, J., and Nägler, T.F., 2003, Model for kinetic effects on calcium isotope fractionation (δ^{44}Ca) in inorganic aragonite and cultured planktonic foraminifera: Geochimica et Cosmochimica Acta, v. 67, p. 1375–1382, https://doi.org/10.1016/S0016-7037(02)01296-6.

Hall, J.L.O., Newton, R.J., Witts, J.D., Francis, J.E., Hunter, S.J., Jamieson, R.A., Harper, E.M., Crame, J.A., and Haywood, A.M., 2018, High benthic methane flux in low sulfate oceans: Evidence from carbon isotopes in Late Cretaceous Antarctic bivalves: Earth and Planetary Science Letters, v. 497, p. 113–122, https://doi.org/10.1016/j.epsl.2018.06.014.

Heinemann, A., Fietzke, J., Melzner, F., Böhm, F., Thomsen, J., Garbe-Schönberg, D., and Eisenhauer, A., 2012, Conditions of *Mytilus edulis* extracellular body fluids and shell composition in a pH-treatment experiment: Acid-base status, trace elements and δ^{11}B: Geochemistry Geophysics Geosystems, v. 13, Q01005, https://doi.org/10.1029/2011GC003790.

Henehan, M.J., Hull, P.M., Penman, D.E., Rae, J.W.B., and Schmidt, D.N., 2016, Biogeochemical significance of pelagic ecosystem function: An end-Cretaceous case study: Philosophical Transactions of the Royal Society of London, ser. B, Biological Sciences, v. 371, p. 20150510, https://doi.org/10.1098/rstb.2015.0510.

Higgins, J.A., et al., 2018, Mineralogy, early marine diagenesis, and the chemistry of shallow-water carbonate sediments: Geochimica et Cosmochimica Acta, v. 220, p. 512–534, https://doi.org/10.1016/j.gca.2017.09.046.

Hippler, D., Witbaard, R., van Aken, H.M., Buhl, D., and Immenhauser, A., 2013, Exploring the calcium isotope signature of *Arctica islandica* as an environmental proxy using laboratory- and field-cultured specimens: Palaeogeography, Palaeoclimatology, Palaeoecology, v. 373, p. 75–87, https://doi.org/10.1016/j.palaeo.2011.11.015.

Hönisch, B., et al., 2012, The geological record of ocean acidification: Science, v. 335, p. 1058–1063, https://doi.org/10.1126/science.1208277.

Huber, B.T., 1988, Upper Campanian–Paleocene foraminifera from the James Ross Island region, Antarctic Peninsula, *in* Feldmann, R.M., and Woodburne, M.O., eds., Geology and Paleontology of Seymour Island Antarctic Peninsula: Geological

Society of America Memoir 169, p. 163–252, https://doi.org/10.1130/MEM169-p163.
Keller, G., Abramovich, S., Berner, Z., and Adatte, T., 2009, Biotic effects of the Chicxulub impact, K-T catastrophe and sea level change in Texas: Palaeogeography, Palaeoclimatology, Palaeoecology, v. 271, p. 52–68, https://doi.org/10.1016/j.palaeo.2008.09.007.
Kısakürek, B., Eisenhauer, A., Böhm, F., Hathorne, E.C., and Erez, J., 2011, Controls on calcium isotope fractionation in cultured planktic foraminifera, *Globigerinoides ruber* and *Globigerinella siphonifera*: Geochimica et Cosmochimica Acta, v. 75, p. 427–443, https://doi.org/10.1016/j.gca.2010.10.015.
Komar, N., and Zeebe, R.E., 2016, Calcium and calcium isotope changes during carbon cycle perturbations at the end-Permian: Paleoceanography, v. 31, p. 115–130, https://doi.org/10.1002/2015PA002834.
Lasaga, A.C., Berner, R.A., Garrels, R.M., Sundquist, E.T., and Broecker, W.S., 1985, An improved geochemical model of atmospheric CO_2 fluctuations over the past 100 million years, *in* Sundquist, E.T., and Broecker, W.S., eds., The Carbon Cycle and Atmospheric CO_2: Natural Variations Archean to Present: American Geophysical Union Geophysical Monograph 32, p. 397–411, https://doi.org/10.1029/GM032p0397.
Lehn, G.O., Jacobson, A.D., and Holmden, C., 2013, Precise analysis of Ca isotope ratios ($\delta^{44/40}$Ca) using an optimized ^{43}Ca–^{42}Ca double-spike MC-TIMS method: International Journal of Mass Spectrometry, v. 351, p. 69–75, https://doi.org/10.1016/j.ijms.2013.06.013.
Lyson, T.R., Bercovici, A., Chester, S.G.B., Sargis, E.J., Pearson, D., and Joyce, W.G., 2011, Dinosaur extinction: Closing the '3 m gap': Biology Letters, v. 7, p. 925–928, https://doi.org/10.1098/rsbl.2011.0470.
Macellari, C.E., 1988, Stratigraphy, sedimentology, and paleoecology of Upper Cretaceous/Paleocene shelf-deltaic sediments of Seymour Island, *in* Feldmann, R.M., and Woodburne, M.O., eds., Geology and Paleontology of Seymour Island Antarctic Peninsula: Geological Society of America Memoir 169, p. 25–54, https://doi.org/10.1130/MEM169-p25.
Marriott, C.S., Henderson, G.M., Belshaw, N.S., and Tudhope, A.W., 2004, Temperature dependence of δ^7Li, δ^{44}Ca and Li/Ca during growth of calcium carbonate: Earth and Planetary Science Letters, v. 222, p. 615–624, https://doi.org/10.1016/j.epsl.2004.02.031.
McArthur, J.M., Thirlwall, M.F., Engkilde, M., Zinsmeister, W.J., and Howarth, R.J., 1998, Strontium isotope profiles across K/T boundary sequences in Denmark and Antarctica: Earth and Planetary Science Letters, v. 160, p. 179–192, https://doi.org/10.1016/S0012-821X(98)00058-2.
Mejía, L.M., Paytan, A., Eisenhauer, A., Böhm, F., Kolevica, A., Bolton, C., Méndez-Vicente, A., Abrevaya, L., Isensee, K., and Stoll, H., 2018, Controls over $\delta^{44/40}$Ca and Sr/Ca variations in coccoliths: New perspectives from laboratory cultures and cellular models: Earth and Planetary Science Letters, v. 481, p. 48–60, https://doi.org/10.1016/j.epsl.2017.10.013.
Nielsen, L.C., DePaolo, D.J., and De Yoreo, J.J., 2012, Self-consistent ion-by-ion growth model for kinetic isotopic fractionation during calcite precipitation: Geochimica et Cosmochimica Acta, v. 86, p. 166–181, https://doi.org/10.1016/j.gca.2012.02.009.
Nordt, L., Atchley, S., and Dworkin, S., 2003, Terrestrial evidence for two greenhouse events in the latest Cretaceous: GSA Today, v. 13, no. 12, p. 4–9, https://doi.org/10.1130/1052-5173(2003)013<4:TEFTGE>2.0.CO;2.
O'Connell, S.B., 1990, Variations in Upper Cretaceous and Cenozoic calcium carbonate percentages, Maud Rise, Weddell Sea, Antarctica, *in* Barker, P.F., Kennett, J.P., et al., Proceedings of the Ocean Drilling Program, Scientific Results Volume 113: College Station, Texas, Ocean Drilling Program, p. 971–984.
Payne, J.L., Turchyn, A.V., Paytan, A., DePaolo, D.J., Lehrmann, D.J., Yu, M., and Wei, J., 2010, Calcium isotope constraints on the end-Permian mass extinction: Proceedings of the National Academy of Sciences of the United States of America, v. 107, p. 8543–8548, https://doi.org/10.1073/pnas.0914065107.
Petersen, S.V., Dutton, A., and Lohmann, K.C., 2016, End-Cretaceous extinction in Antarctica linked to both Deccan volcanism and meteorite impact via climate change: Nature Communications, v. 7, p. 12079, https://doi.org/10.1038/ncomms12079.
Ridgwell, A., and Zeebe, R.E., 2005, The role of the global carbonate cycle in the regulation and evolution of the Earth system: Earth and Planetary Science Letters, v. 234, p. 299–315, https://doi.org/10.1016/j.epsl.2005.03.006.
Schoene, B., Eddy, M.P., Samperton, K.M., Keller, C.B., Keller, G., Adatte, T., and Khadri, S.F.R., 2019, U-Pb constraints on pulsed eruption of the Deccan Traps across the end-Cretaceous mass extinction: Science, v. 363, p. 862–866, https://doi.org/10.1126/science.aau2422.
Schoepfer, S.D., Tobin, T.S., Witts, J.D., and Newton, R.J., 2017, Intermittent euxinia in the high-latitude James Ross Basin during the latest Cretaceous and earliest Paleocene: Palaeogeography, Palaeoclimatology, Palaeoecology, v. 477, p. 40–54, https://doi.org/10.1016/j.palaeo.2017.04.013.
Schulte, P., et al., 2010, The Chicxulub asteroid impact and mass extinction at the Cretaceous-Paleogene boundary: Science, v. 327, p. 1214–1218, https://doi.org/10.1126/science.1177265.
Sprain, C.J., Renne, P.R., Clemens, W.A., and Wilson, G.P., 2018, Calibration of chron C29r: New high-precision geochronologic and paleomagnetic constraints from the Hell Creek region, Montana: Geological Society of America Bulletin, v. 130, p. 1615–1644, https://doi.org/10.1130/B31890.1.
Sprain, C.J., Renne, P.R., Vanderkluysen, L., Pande, K., Self, S., and Mittal, T., 2019, The eruptive tempo of Deccan volcanism in relation to the Cretaceous-Paleogene boundary: Science, v. 363, p. 866–870, https://doi.org/10.1126/science.aav1446.
Tang, J., Dietzel, M., Böhm, F., Köhler, S.J., and Eisenhauer, A., 2008, Sr^{2+}/Ca^{2+} and $^{44}Ca/^{40}Ca$ fractionation during inorganic calcite formation: II. Ca isotopes: Geochimica et Cosmochimica Acta, v. 72, p. 3733–3745, https://doi.org/10.1016/j.gca.2008.05.033.
Tobin, T.S., 2017, Recognition of a likely two phased extinction at the K-Pg boundary in Antarctica: Scientific Reports, v. 7, p. 16317, https://doi.org/10.1038/s41598-017-16515-x.
Tobin, T.S., Ward, P.D., Steig, E.J., Olivero, E.B., Hilburn, I.A., Mitchell, R.N., Diamond, M.R., Raub, T.D., and Kirschvink, J.L., 2012, Extinction patterns, δ^{18}O trends, and magnetostratigraphy from a southern high-latitude Cretaceous–Paleogene section: Links with Deccan volcanism: Palaeogeography, Palaeoclimatology, Palaeoecology, v. 350–352, p. 180–188, https://doi.org/10.1016/j.palaeo.2012.06.029.
Tyrrell, T., Merico, A., and McKay, D.I.A., 2015, Severity of ocean acidification following the end-Cretaceous asteroid impact: Proceedings of the National Academy of Sciences of the United States of America, v. 112, no. 21, p. 6556–6561, https://doi.org/10.1073/pnas.1418604112.
Wallmann, K., 2001, Controls on the Cretaceous and Cenozoic evolution of seawater composition, atmospheric CO_2 and climate: Geochimica et Cosmochimica Acta, v. 65, p. 3005–3025, https://doi.org/10.1016/S0016-7037(01)00638-X.
Westerhold, T., Röhl, U., Donner, B., McCarren, H.K., and Zachos, J.C., 2011, A complete high-resolution Paleocene benthic stable isotope record for the central Pacific (ODP Site 1209): Paleoceanography, v. 26, PA2216, https://doi.org/10.1029/2010PA002092.
Witts, J.D., Bowman, V.C., Wignall, P.B., Alistair Crame, J., Francis, J.E., and Newton, R.J., 2015, Evolution and extinction of Maastrichtian (Late Cretaceous) cephalopods from the López de Bertodano Formation, Seymour Island, Antarctica: Palaeogeography, Palaeoclimatology, Palaeoecology, v. 418, p. 193–212, https://doi.org/10.1016/j.palaeo.2014.11.002.
Witts, J.D., Whittle, R.J., Wignall, P.B., Crame, J.A., Francis, J.E., Newton, R.J., and Bowman, V.C., 2016, Macrofossil evidence for a rapid and severe Cretaceous-Paleogene mass extinction in Antarctica: Nature Communications, v. 7, p. 11738, https://doi.org/10.1038/ncomms11738.
Zinsmeister, W.J., 2001, Late Maastrichtian short-term biotic events on Seymour Island, Antarctic Peninsula: The Journal of Geology, v. 109, p. 213–229, https://doi.org/10.1086/319239.

Printed in USA